Interactions in Shaken Lattice Interferometry

by

Alana Press

University of Colorado at Boulder

Department of Applied Mathematics

Defended April 11th, 2023

Thesis Advisor:

Murray Holland, Department of Physics

Committee Members:

Bethany Wilcox, Department of Physics

Anne Dougherty, Department of Applied Mathematics

Jonathan Kish, Department of Applied Mathematics

Press, Alana (B.S., Applied Mathematics)

Interactions in Shaken Lattice Interferometry

Thesis directed by Prof. Murray Holland

Precision sensing and measurement is of fundamental importance to any scientific endeavor. As technologies have advanced, measurements have reached the precipice of quantum limited sensing. As a result of this rapid advancement, the field of quantum metrology has become a distinct and important field of physics research. Recently, major advancements in quantum technology have created the opportunity that, in the near future, simple quantum mechanical devices may be used to probe extreme physics via tabletop experiment [2]. Specifically, matter-wave interferometry is an area of interest due to its potential for accurate measurements of a myriad of fields, forces, and interactions [5]. In direct analogue to optical interferometry, matter-wave interferometry uses the principle of coherently splitting and recombining a wave to measure the difference in the lengths of the paths taken. The key difference is that matter-wave interferometry uses massive particles instead of light. The smaller de Broglie wavelengths of particles allow for more precise measurements compared to those of light, at the cost of added complexities through interaction. Additionally, massive particles are subject to gravity and can sense inertial changes that photons can't. Although matter may have a theoretical edge over light, there has not yet been an experimental matter-wave interferometer that surpasses the best optical interferometer in accuracy. The use of a precisely controlled shaken lattice provides a completely new pathway for realizing matter-wave interferometry and may generating higher fidelities and precision [4] than otherwise achievable through conventional means.

Although shaken lattice interferometry has been shown to be an accurate and effective method for small atomic systems, there is a downside in its ability to scale to larger atomic ensembles. When the lattice is loaded with a bosonic gas on the order of 50,000 atoms, atomic interactions become important. In this thesis, I will discuss the mean field effects of this gas in the lattice, and how

to control these effects to improve upon existing matter-wave inteferometry. I do this by using the Gross-Pitaevskii equation to describe the interacting wave-function evolution. Then, I use existing shaking functions derived for a noninteracting system in a fully interacting simulation to model these effects in the current configuration of experiments. I improve upon these methods in the presence of interaction by using the interacting model to learn new shaking functions, whereupon I compare and contrast how they behave in interacting and non-interacting models. Finally, I show how these models can be used to precisely measure a simulated constant acceleration similar to gravity.

Dedication

To Jayne Everson.

Acknowledgements

I would like to thank Murray Holland, Jarrod Reilly, and John Wilson for all your help and encouragement. I would also like to thank my parents, Kate Stelwagon, and Rebekah Morrison for your support throughout this process. I would like to thank Jonathan Kish for all of your guidance. I would also like to thank Don Wilkerson for your help writing and editing.

Contents

Tables

Table

Figures

Figure

10

Chapter 1

Introduction

Recent advances in laser cooling and trapping of atoms and molecules have allowed the field of precision metrology to use quantum measurements with unprecedented size and control. In matter-wave interferometry, the measurement result depends on the phase difference accumulated between two de Broglie waves that propagate along spatially separated paths, where each path is associated to a specific value of atomic momentum. Compared with optical interferometers, where the photon wavelength is constrained to be in the vicinity of the visible spectrum, the de Broglie wavelength of atoms can be made small simply by accelerating them. This offers the potential to produce measurement devices in which the interference patterns contain detailed structures at a scale well below a typical optical wavelength. Matter-wave interferometry, in particular atom interferometry, theoretically enables precision measurements of extremely small fields and inertial perturbations. Employing atoms is of fundamental interest since, unlike their light-wave counterparts, the atoms are massive and therefore the interferometer's signal is sensitive to gravitational as well as inertial phase shifts. Such sensitivity could allow navigation in GPS-free environments and multiple remote sensing applications such as navigation and groundwater mapping [10].

Although the physical nature of matter-waves may potentially have a theoretical edge over optical waves, a matter-wave interferometer with higher quantum sensitivity than their optical counterparts has not yet been realized. Optical waves with an enormous flux of photons are much easier to deploy experimentally through the use of lasers. On the other hand, current matter-wave interferometry schemes rely on the use of small ensembles of ultra-cold atoms that are well described

by single particle physics. The single particle model is simple in theory, but only an approximation to the real many-body systems relevant to experiment. In this thesis, I will discuss the effects of the particle-particle interactions at the first level of perturbation theory and the validity of the non-interacting assumption. Furthermore, I will show solutions to shaking functions that account for interactions. The fundamental component needed to construct a shaken lattice interferometer is an optical lattice. The optical lattice is the basis of today's most precise quantum instrument: an atomic clock that utilizes ultra-cold atoms confined in a three-dimensional optical lattice that has achieved timekeeping uncertainty on the order of 10^{-19} [2] The optical lattice clock is a million times more precise than the cesium clocks that keep the world's time. I show that this precise atomic system may be extended and used as a framework for matter-wave intereferometry that is capable of measuring not time but inertial forces.

In optical interferometry, device components including beamsplitters and mirrors control the splitting, reflecting, and recombining of the optical wave. Shaken lattice matter-wave interferometry requires that the lattice be shaken in a specific way in order to split, reflect, and recombine the matter-wave. These shaking functions are often unintuitive, and thus will be derived via reinforcement machine learning. To date, these shaking functions have only been found for non-interacting wave function evolution [4]. Applying an interacting model to the shaken lattice scheme would incorporate the inevitable effects of the mean-field interaction, and may improve the fidelity and increase the precision achieved by a fully quantum limited matter-wave interferometer.

In this thesis, I take mean-field interactions into account when generating shaking functions and simulating the resulting shaken lattice interferometer. In Chapter 2, I provide background on shaken lattice matter-wave interferometry, Bose Einstein Condensates, and reinforcement learning. In Chapter 3, I state the problem layout. In Chapter 4, I discuss the interacting and non-interacting beamsplitter shaking functions. In Chapter 5, I discuss the effects of interactions on the mirror function. In Chapter 6, I show the cascading of these components to form a complete interferometer sequence and demonstrate their use for measuring accelerations. Finally, in Chapter 7, I discuss the conclusions and potential next steps of this research.

Chapter 2

Background

Interferometry has been an important tool in precision metrology for decades. By leveraging the quantum nature of light and matter, we have been able to measure phenomena on micro and macroscopic scales [6, 1]. Recently, there has been an emphasis on matter-wave interferometry because of its theoretical ability to produce extremely detailed interference patterns and sense inertial changes.

2.1 Matter-Wave Interferometry

The simplest matter-wave interferometer uses the same general scheme as the optical double slit interferometer. As shown in fig. 2.1, atoms from a source pass through a double slit, travel along two distinct paths, and recombine via a single slit [3]. The quantum mechanical nature of small particles, like the helium atom, is used to replace optical waves with matter-waves. Since the

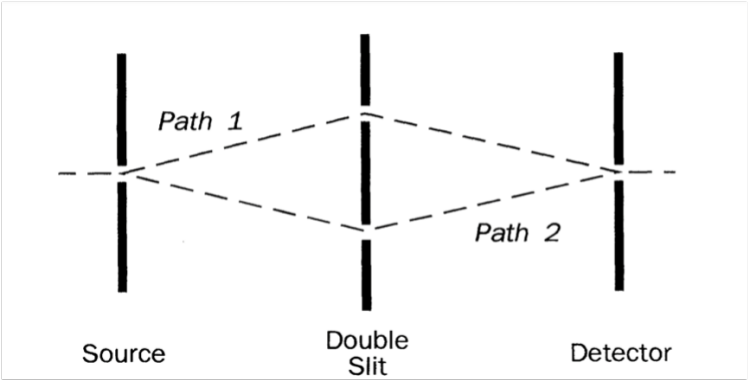

Figure 2.1: Optical double slit interferometer scheme.[3]

two-path scheme, matter-wave interferometry has advanced to include more complicated schemes. Modern matter-wave interferometers have split larger particles and increased fidelity by using laser pulses. The resonant absorption and emission processes alter the energy and momentum of the matter-wave and cause it to coherently split into two components. The subsequent recombination causes interference in the manner of optical wave interference. This interference, which manifests as a fringe, is the measurement output of the interferometer. The phase of the wavefunction depends on the integrated energy of the particle computed over the distance of the path it travels. Thus, the interference between the two matter waves depends on the difference in these accumulated phases, which is a property of the path length difference.

In a matterwave interferometer with a single atom, the wavefunction is first split into two momenta by the beam splitter; $|\psi(t=0)\rangle = (|+n\hbar k\rangle + |-n\hbar k\rangle)/\sqrt{2}$, where k is the wavenumber corresponding to the de Broglie wavelength. Each branch of the wavefunction travels along path one (with $p = +n\hbar k$) or path two (with $p = -n\hbar k$). As the atom travels, it is subject to the hamiltonian

$$\hat{H} = \frac{\hat{p}^2}{2m} + ma\hat{x}, \tag{2.1}$$

where m is the atomic mass, a is the acceleration due to gravity, and the operators $\hat{p}$ and $\hat{x}$ are momentum and position of the atom, respectively. By taking an interaction picture that is co-falling with the atoms one finds

$$\begin{aligned} \hat{H}_{\text{Int}}(t) =& \frac{(\hat{p} - mat)^2}{2m}, \\ =& \frac{\hat{p}^2}{2m} - at\hat{p} + (mat)^2, \end{aligned} \tag{2.2}$$

where the non-operator terms have been dropped. From this Hamiltonian, the time evolution is given by $\exp\left(-\frac{i}{\hbar}\int_0^t \hat{H}(s)ds\right)|\psi(t=0)\rangle$, and the relative phase may be directly calculated via

$$\begin{aligned} \phi(a,t) =& \frac{-1}{\hbar}\int_0^t ds \left(\langle +n\hbar k|\, \hat{H}(s)\, |+n\hbar k\rangle - \langle -n\hbar k|\, \hat{H}(s)\, |-n\hbar k\rangle\right), \\ =& nkat^2. \end{aligned} \tag{2.3}$$

This relative phase encodes in the interference pattern the value of a, and from this we can use the Heisenberg energy-time uncertainty principle to conclude that:

$$\left(\Delta\hat{H}\right)^2 (\Delta t)^2 = \frac{1}{4}(n\hbar kt)^2 (\Delta a)^2 (\Delta t)^2 \geq \frac{\hbar^2}{4}, \quad \text{implies} \quad (\Delta a)^2 \geq \left(nkt^2\right)^{-2}, \tag{2.4}$$

where it is assumed $\Delta t = t$. This shows the sensitivity of a matter-wave interferometer is proportional to the area of space-time it encloses: $x \cdot t = (vt) \cdot t = nkt^2$, and directly shows the enhancement due to smaller de Broglie wavelengths of atoms since $k = 2\pi/\lambda_{deBroglie}$. It should be noted that this intuitive derivation matches more formal analysis [7] using the Fisher Information. This bound has not yet been saturated in experiment due to the practical challenges of working with BECs.

2.1.1 Shaken Lattice Interferometry

The most important component of a shaken lattice interferometer is an optical lattice. An optical lattice is created by the interference of two counter-propagating lasers and can be one, two, or three dimensional. Atoms at the anti-nodes of the lattice experience a lower potential energy, if the lattice is red detuned from the atomic transition, and can therefore be trapped, as seen in fig. 2.2. To shake the lattice, the phase of the light is modulated with two acoustic-optic modulators, one on each laser. The acoustic-optic modulator is a device that can modulate the characteristics of the light including the phase, frequency, and amplitude of a radio frequency signal injected into the device. Amplitude modulation of the optical lattice can also be used to split, reflect, and recombine particles, although it results in a varying lattice depth that is not a simple as the one we consider here. Both approaches can cause momentum splitting; the difference between the momenta of the two components of the quantum wavefunction. This method in this paper uses phase modulation, which is referred to as the shaking function and causes particles to split, reflect, and recombine. An illustration of these effects can be seen in fig. 2.3. This process begins with a particle in the ground state which is split into two counter propagating matter-waves. The two waves have the same amplitude and opposite momenta of $\pm 2n\hbar k$, where n refers to the

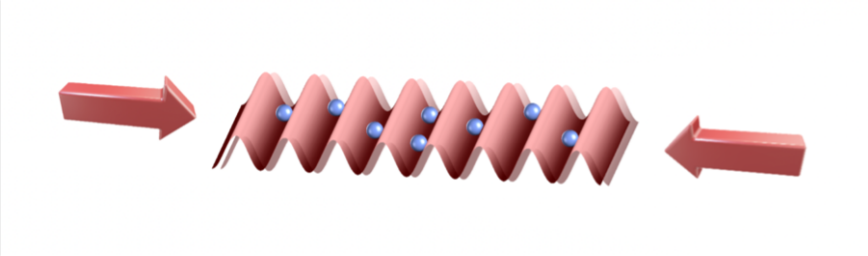

Figure 2.2: Optical lattice loaded with bosons. [4]

number of photon interactions and k is the wave number. Although it is very difficult to achieve $4\hbar k$ splitting via convectional matter-waver interferometry methods, the shaken lattice method has shown the ability to easily achieve momentum splitting of $8\hbar k$ [4]. Note that the quantization of the momentum remains the same for the shaken lattice method due to the fundamental $\lambda/2$ periodicity of the wells of the lattice where λ is the optical wavelength. The momentum spread is an important factor in the accuracy of the interferometer, because it is inversely proportional to the wavelength. Shorter wavelengths cause more detailed interference patterns and a more sensitive interferometer.

2.2 Bose Einstein Condensates

A Bose Einstein Condensates (BEC) is a gas of bosonic particles where each boson is in the same quantum state. This is achieved by cooling the gas below a critical temperature near absolute zero, which results in a macroscopic fraction of the bosons being in the ground state. The property that all of the bosons in the BEC are in the same quantum states means that the gas can be modeled at the mean-field level. Modeling at the mean-field level means that one single-particle wave function can describe the entire ensemble. A typical BEC achievable in laboratory settings contains up to 100,000 particles, and thus particle-particle interactions are impossible to avoid. For this reason, modeling the effects of these interactions on the shaking functions is of interest. Prior to my work, the one dimensional Schrödinger equation,

$$\frac{\partial}{\partial t}\left|\psi(t)\right\rangle = -\frac{i}{\hbar}\hat{H}\left|\psi(t)\right\rangle, \quad \hat{H}(x,t) = -\frac{\hbar^2}{2m}\frac{\partial^2}{\partial x^2} + V(x,t) \tag{2.5}$$

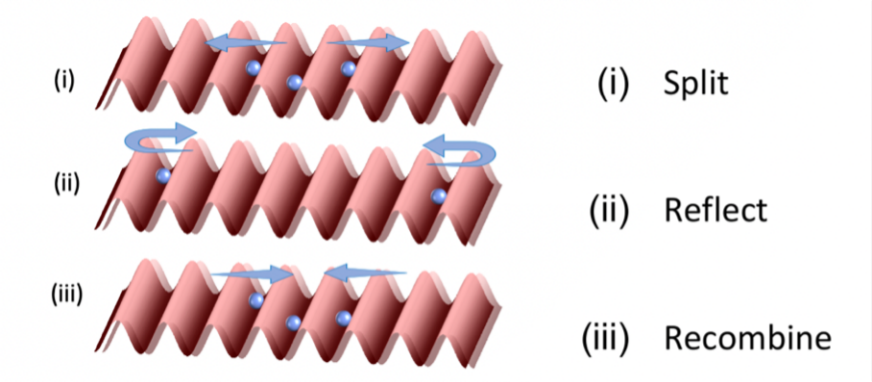

Figure 2.3: Phase modulation in the lattice causing splitting, reflecting, and recombining of atoms.[4]

has been used for this purpose, where $V(x,t)$ contains the lattice and gravitational potential energy contributions. The Schrödinger equation does not include any particle-particle interactions. In this thesis, I use a Hamiltonian of the form

$$\hat{H}(x,t) = -\frac{\hbar^2}{2m}\frac{\partial^2}{\partial x^2} + V(x,t) + g|\Psi(x,t)|^2, \tag{2.6}$$

which includes particle-particle interactions at the mean field level and from which the one dimensional Gross-Pitaevskii Equation may be written. The Gross-Pitaevskii equation,

$$i\hbar\frac{\partial}{\partial t}|\psi(x,t)\rangle = (-\frac{\hbar^2}{2m}\frac{\partial^2}{\partial x^2} + V(x,t) + g|\Psi(x,t)|^2)\,|\psi(x,t)\rangle\,, \tag{2.7}$$

is nonlinear because of the third term in the Hamiltonian, which contains ψ. When the model includes particle interactions, the matter-waves correspond to collective excitations of the BEC.

2.2.1 Experimental production

Experimentally, BECs are created by cooling bosons to extremely low temperatures, typically around 100 nK. The bosons are obtained from a dispenser source that expels atoms such as Rubidium-87. A typical BEC begins by capturing atoms in a magneto-optical trap (MOT). The MOT works by using laser cooling to slow atoms and a magnetic field to contain the atoms. BECs are short-lived in experiments because they typically decay through inelastic processes.

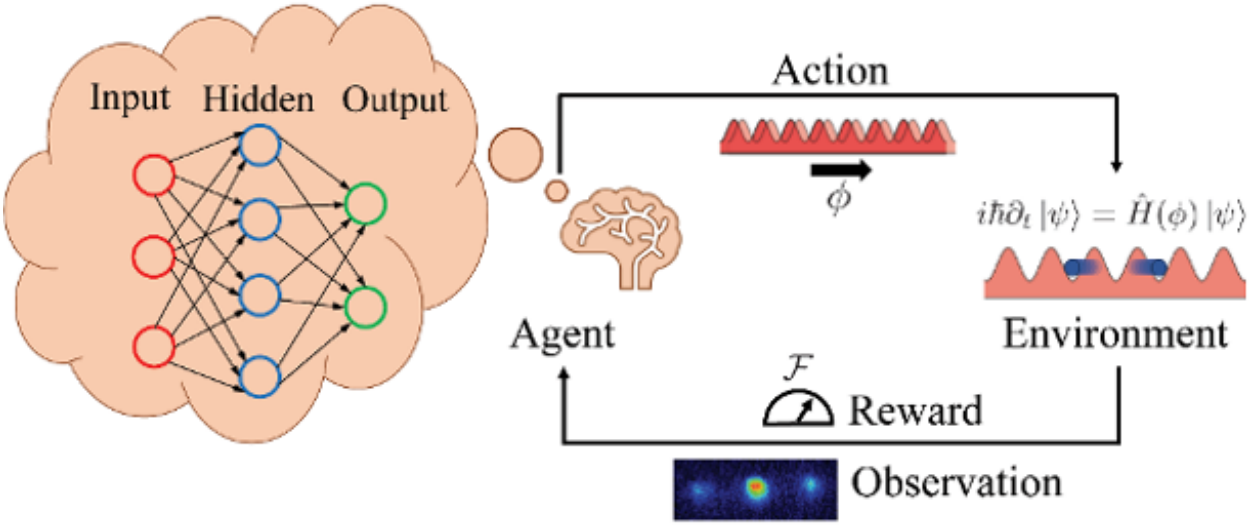

Figure 2.4: Reinforcement learning cycle.[4]

2.3 Reinforcement-learning

Reinforcement-learning is a type of machine learning that uses simulations or data to determine the best solution to a problem. The method executes actions on an environment and uses trial and error to determine the best output to optimize the outcome. Fig. 2.4 illustrates this method, showing the cycle in which an action in implemented by the agent and the resulting effect on the environment returns a reward to the agent. A benefit of this type of machine learning is that it decreases human bias in the decision-making process. A result of this lack of bias is that the algorithm can come up with unintuitive solutions that humans would not likely think of. For example, reinforcement-learning is effective at playing chess and often executes moves which have a negative effect in the short term but eventually win the game. It is also useful in complex problems where run of the mill algorithms are ineffective or take too much time. These characteristics make reinforcement-learning extremely effective in quantum design and a useful tool in shaken lattice interferometry.

2.3.1 Environment

The environment is a mathematical model of the problem in which the actions are performed and where the design takes place. It is important to note that the environment does not need to be completely understood or completely modeled, it only needs to be described in such a way to be able to produce observables which determine the reward associated with the actions. In the application of a shaken lattice interferometer with excitations, the environment is the BEC in the lattice potential. The model described above is used to determine the state of the BEC in the current lattice position.

2.3.2 Action

Actions in this framework are phase shifts of the lattice. One action may change the phase by some amount less than the spatial period, which therefore causes the nodes of the lattice to move. The learning algorithm is called a Markov decision process, which means that the state of the environment is determined only by the current state of the system and current action, not by the past history. The number of actions is a parameter in the design of the algorithm. The algorithm has a terminal condition which, when reached, determines that no more actions will be taken. This terminal condition may be some feature of the system (such as a threshold performance metric), a desired number of actions, or a combination of both. The terminal action may be adjusted to improve the learning scheme.

2.3.3 Agent and hidden layers

The agent is the neural network that decides the actions. The agent is given a state vector which contains relevant features of the environment. Given these features, the agent outputs a vector of quality factors which are called the Q-values. The Q-values are a function of the input state vector and possible actions. Each Q-value is an estimate of the quality of the action given the current state by comparing the result of the action with the desired target of the algorithm. Thus, the highest Q-value corresponds to the most desirable action. The agent executes the action

associated with the highest Q-value which updates the environment and determines a new state.

2.3.4 Observation and Reward

After taking an action, the agent observes the outcome and a reward is given back to the agent based on the effectiveness of the action that was chosen. The return is defined as the combination of both current and future rewards. Since the desired outcome is the end result of the algorithm, not the individual steps, the current reward is weighted lower than future rewards. The future reward is determined by the highest Q value of the subsequent action.

2.3.5 Epsilon Greedy

An epsilon-greedy policy prevents the algorithm from choosing the action associated with the highest Q-value every time. Instead, the algorithm has the probability of epsilon of choosing a random action. This forces the agent to explore a wider range of actions and prevents it from being locked into a local solution. The epsilon-greedy policy allows the learning algorithm to weigh exploration versus optimization.

Chapter 3

Problem Layout

3.1 Physical model

The physical model of this problem consists of a Bose Einstein Condensate in a lattice potential. The BEC will be modeled at the mean field level via the Gross-Pitaevskii (GP) equation. The potential is caused by the optical lattice which takes the form of a standing wave. This potential is controlled by the machine learning algorithm to enforce changes to the BEC. The nonlinear term, which incorporates particle-particle interactions according the the scattering length, means that the equation is not analytically solvable. The goal of the problem is to determine the wave equation of the Hamiltonian of the GP equation. To determine the wave equation, a second order ODE must be integrated. I use the fourth order Runge-Kutta iterative method to solve this problem. The Runge-Kutta method requires an initial value, for which I use the ground state of the system. This is physically reasonable since BECs are created with the bosons into the ground state of the system. To determine the ground state, I first find the ground state of the non interacting Hamiltonian by taking the lowest eigenvector of the Hamiltonian matrix. Then, I use imaginary time evolution and repeated re-normalization to determine the interacting ground state. The imaginary time evolution uses the same Runge-Kutta method that I will use to find the time evolution of the system but with an imaginary factor on the time parameter. The imaginary time factor changes the sin and cosine components of the wave equation to real exponential equations with negative exponents. The negative exponents mean that the terms with larger energy values go to zero quickly and the ground state component is amplified. This has the effect of producing a pure representation of

the ground state after many iterations. This interacting ground state becomes the initial value for the Runge-Kutta method to solve the time evolution. We now have a model which can solve the ground state of the Gross-Pitaevskii equation for a BEC in an optical lattice and determine how the wave equation evolves under time-dependent changes to the potential function.

3.2 Computational model

The computational model is the integration of the previously described physical model with a reinforcement machine learning algorithm. This computational model is used to determine the shaking functions for the beamsplitter and mirror of the interferometer. In this section, I will discuss the general structure and interaction between the machine learning algorithm and the physical model. In the next section I will discuss the specific results for the beamsplitter and mirror models. The environment of the reinforcement learning algorithm is the BEC in the optical lattice and is governed by the GP equation. When changes are made to the environment, they are modeled by the methods described above and the new wave equation is determined. The changes to the environment are determined by the actions. The actions here are phase shifts to the optical lattice potential. These phase shifts cause the entire lattice, which we model as infinitely periodic, to shift left or right in our one dimensional model. The shifting left and right is where the name shaken lattice comes from. The actions, phase shifts, are determined by the agent. This is the heart of the machine learning algorithm, which tells us which actions might be productive and determines a learned shaking function. The agent learns which actions may be useful by simulating the environment with each proposed action and observing the reward based on a calculated quantum fidelity. The fidelity is determined by the similarity between the current wave function and a desired wave function, or target. The mathematical expression for this is the modulus squared of the inner product of the wave function and the target. The machine learning cycle runs through many episodes in each trial. During each episode, it chooses an action sequence and observes the terminal reward. If the terminal fidelity increases, the wave function is closer to the target, then it records that action sequence. In addition to the learned strategy, there is

an intentionally introduced element of randomness. This randomness, the epsilon greedy protocol discussed in the background, prevents the agent from focusing to closely to one solution space too quickly and forces it to explore the entire range of action sequences. At the beginning of each trial, the environment is returned to the ground state which was determined by the imaginary time evolution. This process is repeated for a determined number of learning cycles and the best set of actions is returned. Then, the system is simulated to interpret its performance.

Chapter 4

Beamsplitter

The beamsplitter model closely follows the method described in the problem statement. With this method we can find shaking functions for a range of scattering lengths with fidelities above 95%. The most notable difference between this method and previously established methods [4] is the use of position space. We model the lattice and the wave function in position space because it is more straight-forward to solve the Gross-Potaevskii equation this way than in momentum space. The one dimensional Hamiltonian of the system in position space is

$$\hat{H}(x,t) = -\frac{\hbar^2}{2m}\frac{\partial^2}{\partial x^2} + V(x,t) + g|\Psi(x,t)|^2, \tag{4.1}$$

where $V(x,t)$ is the external potential of the lattice, m is the atomic mass, and $g = \frac{4\pi\hbar^2 a}{m}$, where a is the scattering length. We implement periodic boundaries in position space, which also imposes periodic boundary conditions in momentum space. Although the learning algorithm takes place in position space, looking at the position space wave function is not an intuitive way to visualize the effects of the beamsplitter. Thus, most of the plots in this section are in momentum space. I use a fast Fourier transform (FFT) to transform between position and momentum space.

4.1 Lattice and Environment

The lattice potential, modeled in position space for the previously mentioned reasons, is a standing wave that results from the sum of sines and cosines. This potential is modeled as

$$V(x,t) = \sin(\phi) * \sin(2kx) - \cos(\phi) * \cos(2kx), \tag{4.2}$$

where ϕ is the phase of the lattice. The periodic boundary conditions mean that the model only spans one lattice site such that x, in dimensionless lattice units, goes from $-\pi$ to π. To implement these periodic boundary conditions, the kinetic energy term of the Hamiltonian is made to be periodic. The kinetic energy term,

$$-\frac{\hbar^2}{2m}\frac{\partial^2}{\partial x^2}, \tag{4.3}$$

is modeled via numerical finite difference derivative. The periodicity is implemented by mapping the first element, $x = -\pi$, to the last element, $x = \pi$. Phase shifts are modeled as changes to the lattice phase, ϕ. This has the effect of moving the standing wave. To model the effect of this on the wave-function, we need to solve the Gross-Pitaevskii equation.

4.2 Solving the Gross-Pitaevskii Equation

The Gross-Pitaevskii equation is used to determine the effects of the lattice on the wave-function of the BEC. The non-linearity of the Gross-Pitaevskii equation necessitates the use of numerical integration to determine the wave function. As mentioned in the problem statement, the fourth order Runge-Kutta iterative method is used for the numerical integration. We use this method in two ways in this project: real time integration and imaginary time integration.

Real time evolution is used to determine the wave function after each phase shift or action. Physically, this applies the Hamiltonian to the wave function. Computationally, this is implemented as a loop which calls the Runge-Kutta method to compute the numerical time derivative, or the left hand side of the Gross-Pitaevskii equation. During the learning cycle, this happens after each action and is used the calculate the reward. For the beamsplitter, the reward is based on the fidelity, or how close the wave-function is to the target. In this case, the target is the third excited state of the Hamiltonian. This state corresponds to good approximation to $\pm 4\hbar k$ momentum splitting. Larger momentum splittings lead to higher fidelity interferometers, so it would be of interest to use a state with higher momentum splitting in the future.

Imaginary time evolution only occurs once when the lattice is initialized and finds the ground

state wave function. Since the Hamiltonian evolution is comprised of oscillating sin and cos components, if time, t, is replaced with imaginary time, it, the Hamiltonian evolution is instead comprised of decaying exponential functions. The exponents of the different components are proportional to the energy of the state. Thus, exponential functions corresponding to larger energies decay quickly. By re-normalizing during the evolution, the ground state is amplified. This process generates what we call the interacting ground state. This is the ground state of the Hamiltonian of the Gross-Pitaevskii equation which is distinct from the non-interacting ground state, or the ground state of the Schrödinger equation, although, they are similar in shape. We use the fact that they are both smooth and of approximate Gaussian shape to speed up the imaginary time evolution process. We initialize the ground state as the non interacting ground state so that it is closer to the target. The non interacting ground state is easily calculated as the first eigenvector of the Hamiltonian matrix of the Schrödinger equation.

Once the interacting ground state wave function is determined, we use it to calculate the inputs to the learning algorithm. The two main inputs from the environment to the learning algorithm are the reward and a feature, i.e., a reduced representation of the full quantum state. The reward is a function of the fidelity. Since the reward is used to give feedback to the agent, we want to use a function that can clearly distinguish between high and low fidelity. The function we use is

$$\frac{\text{fidelity}}{1-\text{fidelity}}, \tag{4.4}$$

which is zero when the fidelity is zero and approaches infinity when the fidelity approaches one. This results in a very high reward for high fidelity and a very low reward for low fidelity. The feature is defined to be a vector which is comprised of the modulus square of the even and odd parity components of the wave function. This is used by the agent to determine the characteristics of the wave function. A good characteristic to look at in this problem is the evenness and oddness of the wave function. This is useful in differentiating the target wave function from adjacent wave functions that have almost identical energy because the parity alternates with each energy level.

4.3 Testing the Non-Interacting Case

In order to verify that the beamsplitter algorithm does what is intended, we begin by using a scattering length of 0. This puts us in the non-interacting case so the solutions should match what is seen in other verified models that do not account for mean field effects. As can be seen in fig. 4.2, the wave function begins almost entirely in the $0\hbar k$ momentum state, or ground state. By the end of the shaking sequence, the wave function has split into the plus and minus $4\hbar k$ states. It can be seen that there are is some portion of the wave function that is in the surrounding states because the squares are not perfectly dark blue. This is because the fidelity of this beamsplitter shaking function was not 100% so it is not exactly in the target state. The position space wave function, plotted in fig. 4.1, also shows this momentum splitting. The third energy eigenstate, which corresponds to the split momentum space wave function discussed previously, has four peaks over one period of the lattice. The wave function can be seen beginning in the ground state with one peak and ending with four peaks at the end of the shaking sequence, which corresponds to the standing wave with $\pm 4\hbar k$ momentum. This solution matches with the expected results and implies that the model is accurate in the zero scattering case.

4.4 Mean Field Effects on Non-Interacting Shaking Functions

Once the non-interacting case is verified, we can use the interacting model to observe how mean field effects change the fidelity of a beamsplitter solution that was learned on a non-interacting model. Note that the experimental setup that implements these shaking functions is estimated to have an interaction strength on the order of 2 in dimensionless units. As such, I simulated the non-interacting shaking functions in the interacting model with interaction strengths 2, 5, and 10. Note that the interaction strength goes up linearly with the number of atoms in the BEC so if the number of atoms were to double the interaction strength would also double.

It can be seen in table 6.1 that the increasing scattering length decreases the fidelity of the beamsplitter. When the shaking function is simulated with a scattering length of 0, the fidelity of

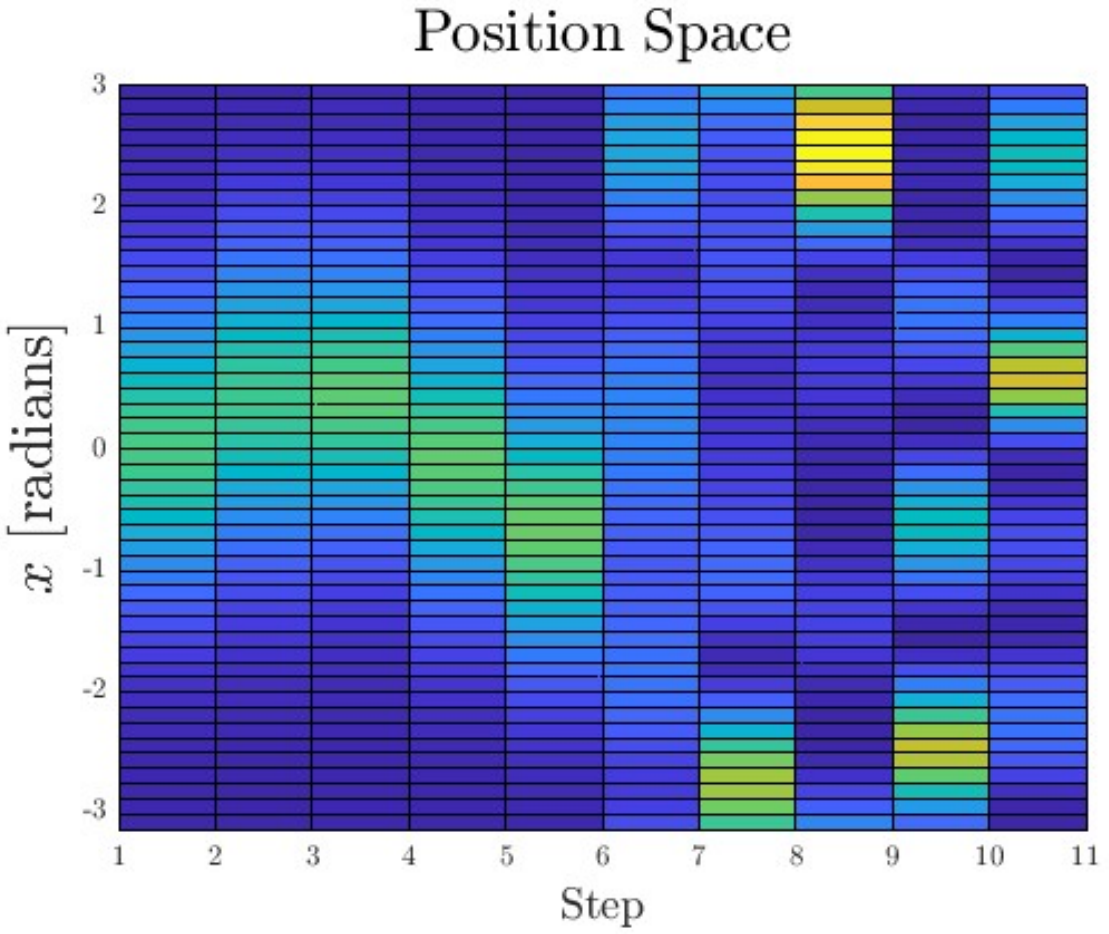

Figure 4.1: Evolution of the position space wave function as a function of time. Time is measured in steps along the x axis. The y axis is the spatial range of the lattice. The color intensity corresponds to the density of the wave function where bright yellow is high density and dark blue is low density.

the beamsplitter is 95.3%. With a scattering length of 2, the fidelity is 94.8%. With a scattering length of 5, the fidelity is 90.5%. With a scattering length of 10, the fidelity is only 60.8%. It is clear that mean field effects are significant in the beamsplitter.

4.5 Learning with the Interacting Model

The shaking function for the interacting beamsplitter is generated in the same way as the non-interacting shaking function but with a non-zero interaction strength. In this thesis, a beamsplitter solution is calculated with a interaction strength of 10 in dimensionless units. The interaction strength scales linearly with the number of atoms in the BEC, and inversely with the number of

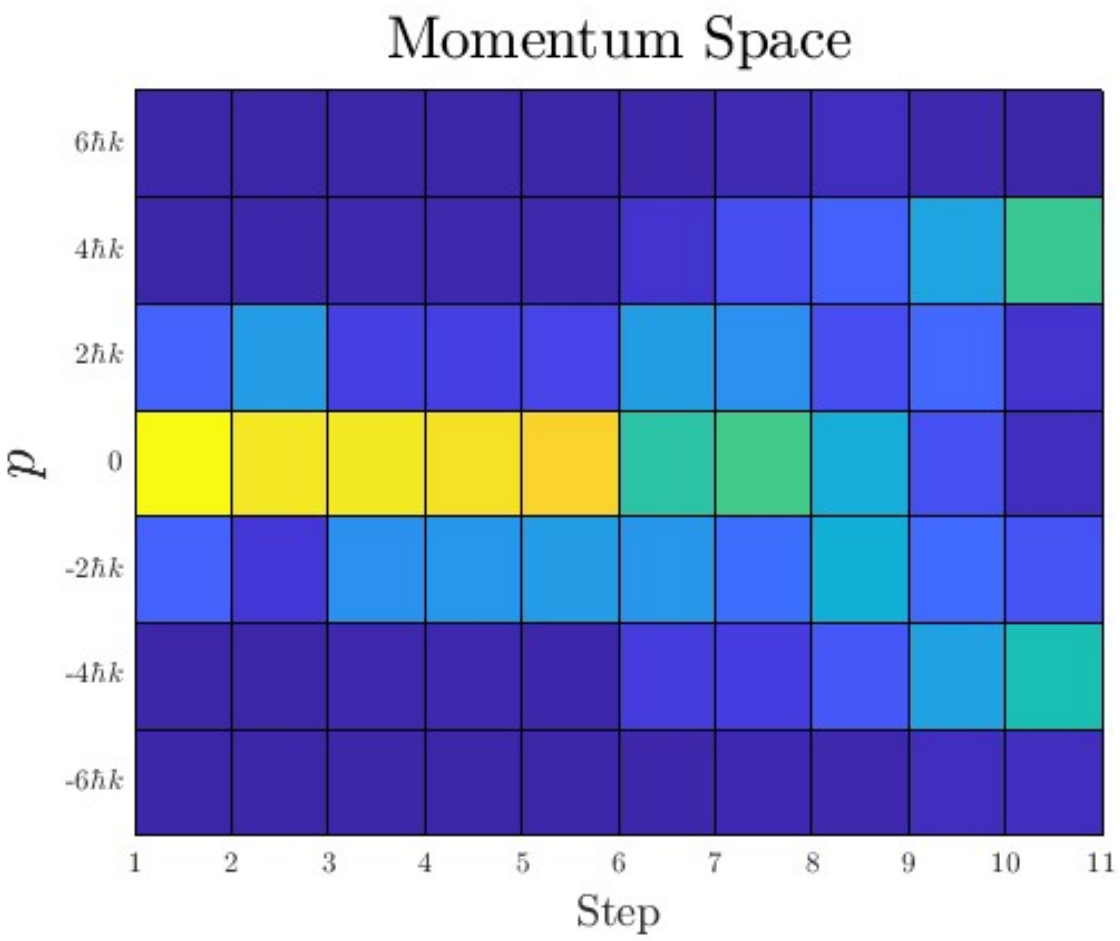

Figure 4.2: Evolution of the momentum space wave function as a function of time. Time is measured in steps along the x axis. The y axis is the momentum range of the wave function. The color intensity corresponds to the density of the wave function where bright yellow is high density and dark blue is low density.

lattice sites occupied. The shaking function is shown in fig. 4.4. It has a fidelity of 97.3%. This shows a promising solution to the problems that arose from interactions on the non-interacting learning function. The learning cycle with interactions does take longer than the non-interacting case because of the numerical integration. As such, the program needs to run for longer to find high fidelity solutions. To achieve 97.3% fidelity, the program ran for around 24 hours. The algorithm could be improved in the future by optimizing the learning parameters, action list, and target state.

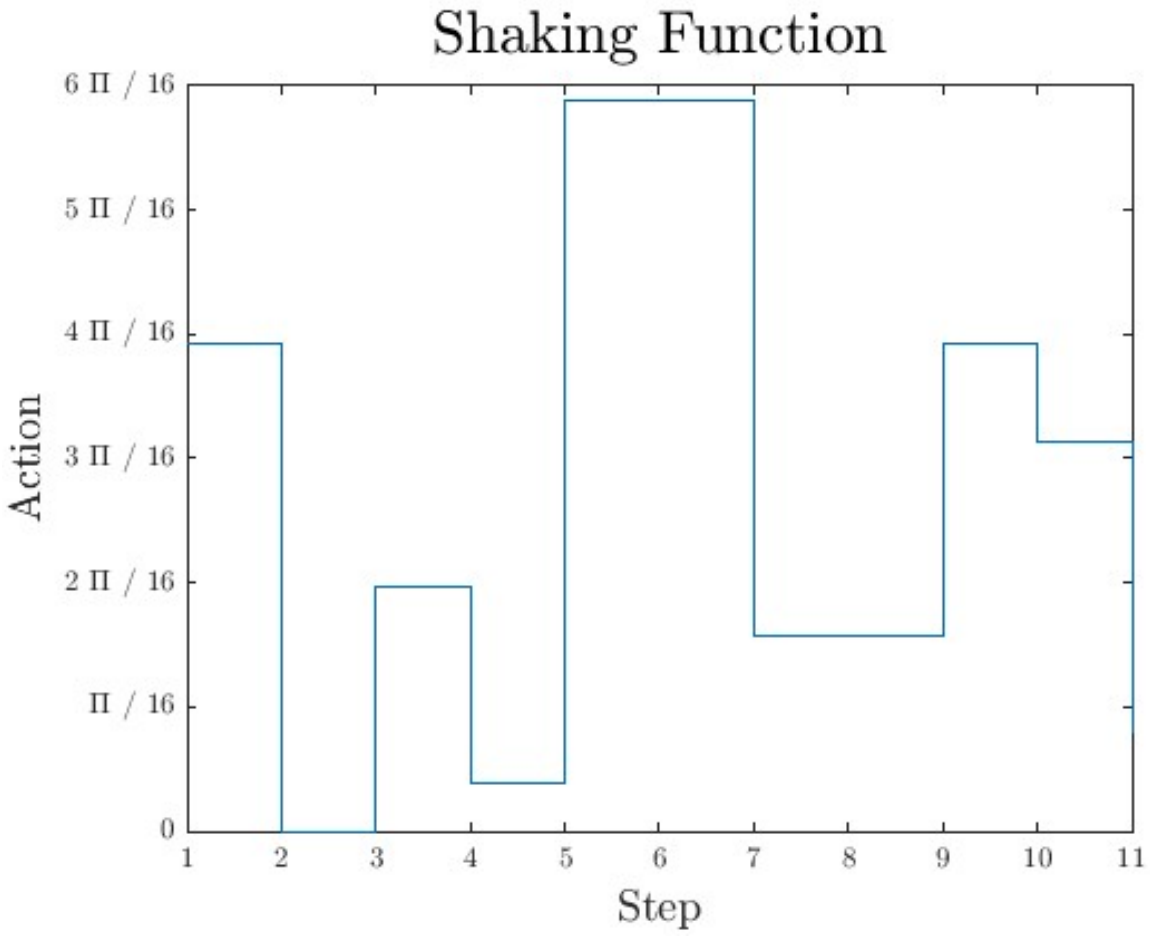

Figure 4.3: Shaking function determined by the reinforcement learning algorithm. The x axis is the step number and the y axis is the phase shift in radians.

	a	b
1	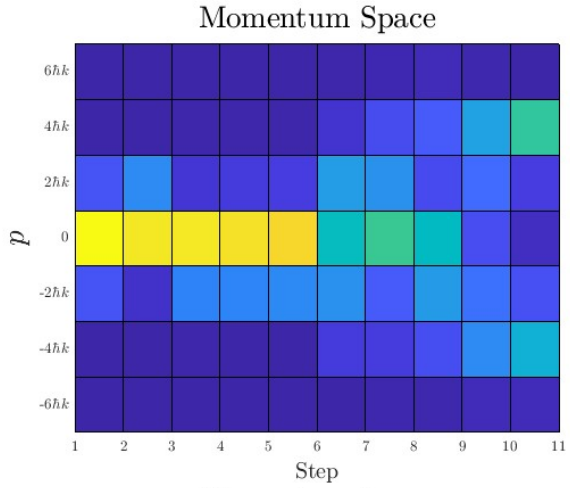	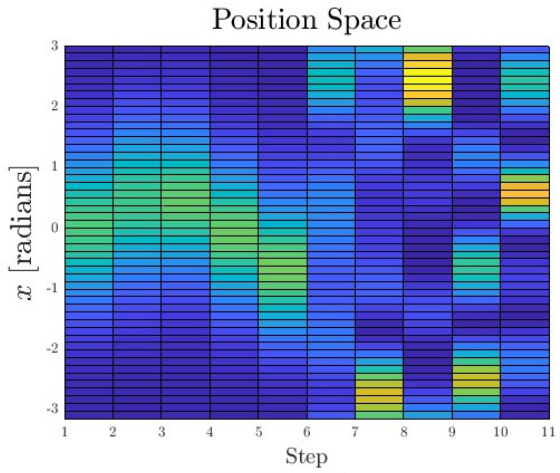
2	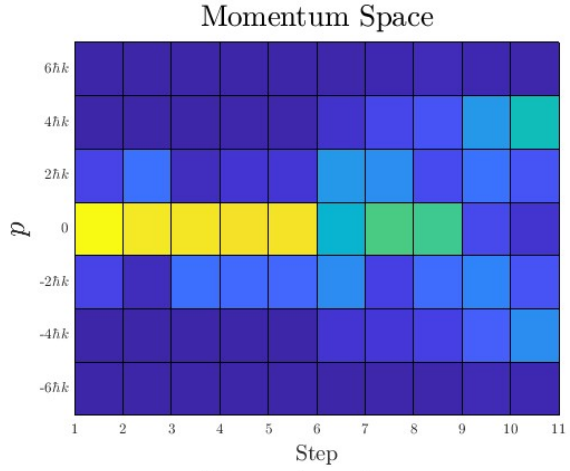	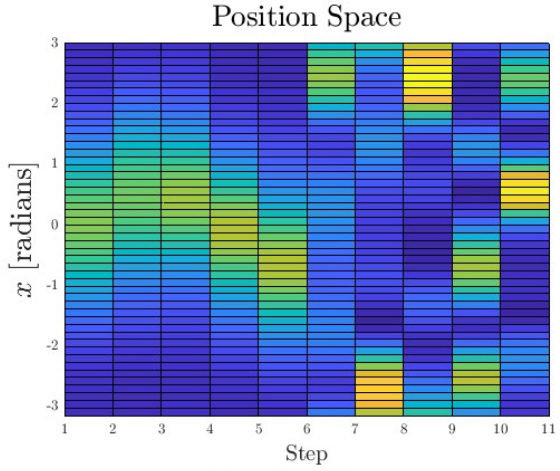
3	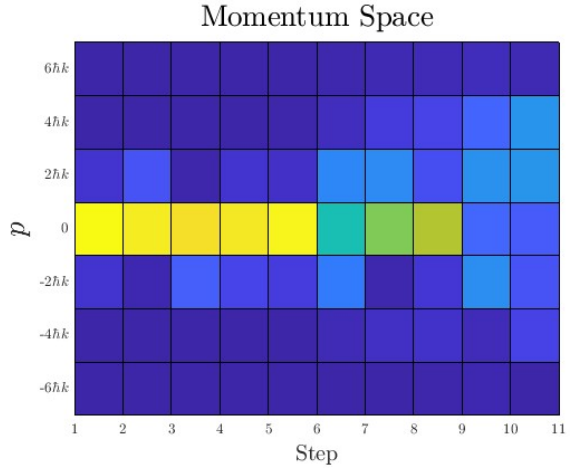	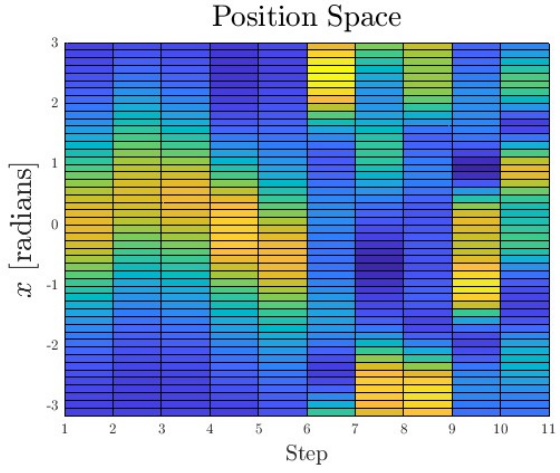

Table 4.1: Non-interacting beamsplitter solution under varying interactions strengths. a) Varying interaction strengths in momentum space. b) Varying interaction strengths in position space. 1) interaction strength 2. 2) Interaction strength 5. 3) Interaction strength 10.

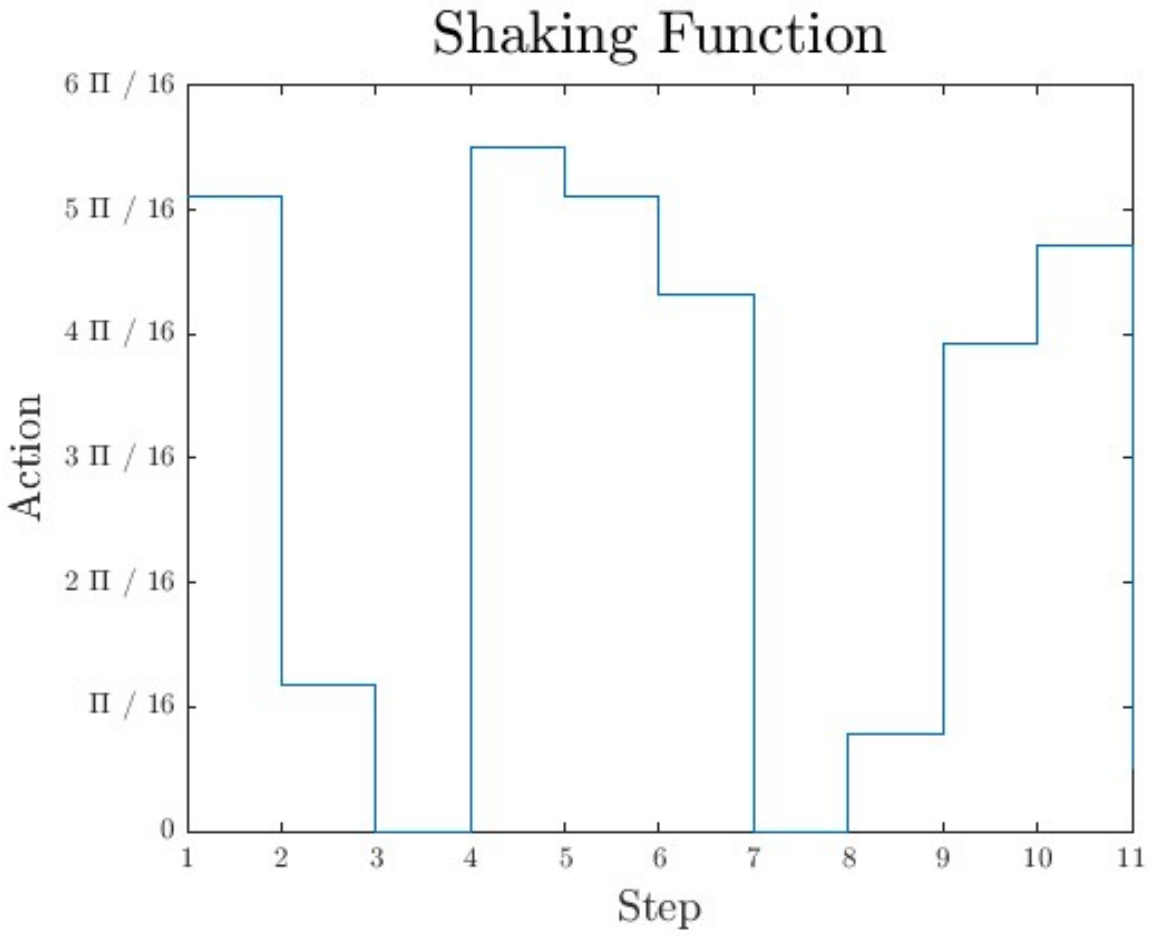

Figure 4.4: Shaking function determined by the reinforcement learning algorithm. The x axis is the step number and the y axis is the phase shift in radians.

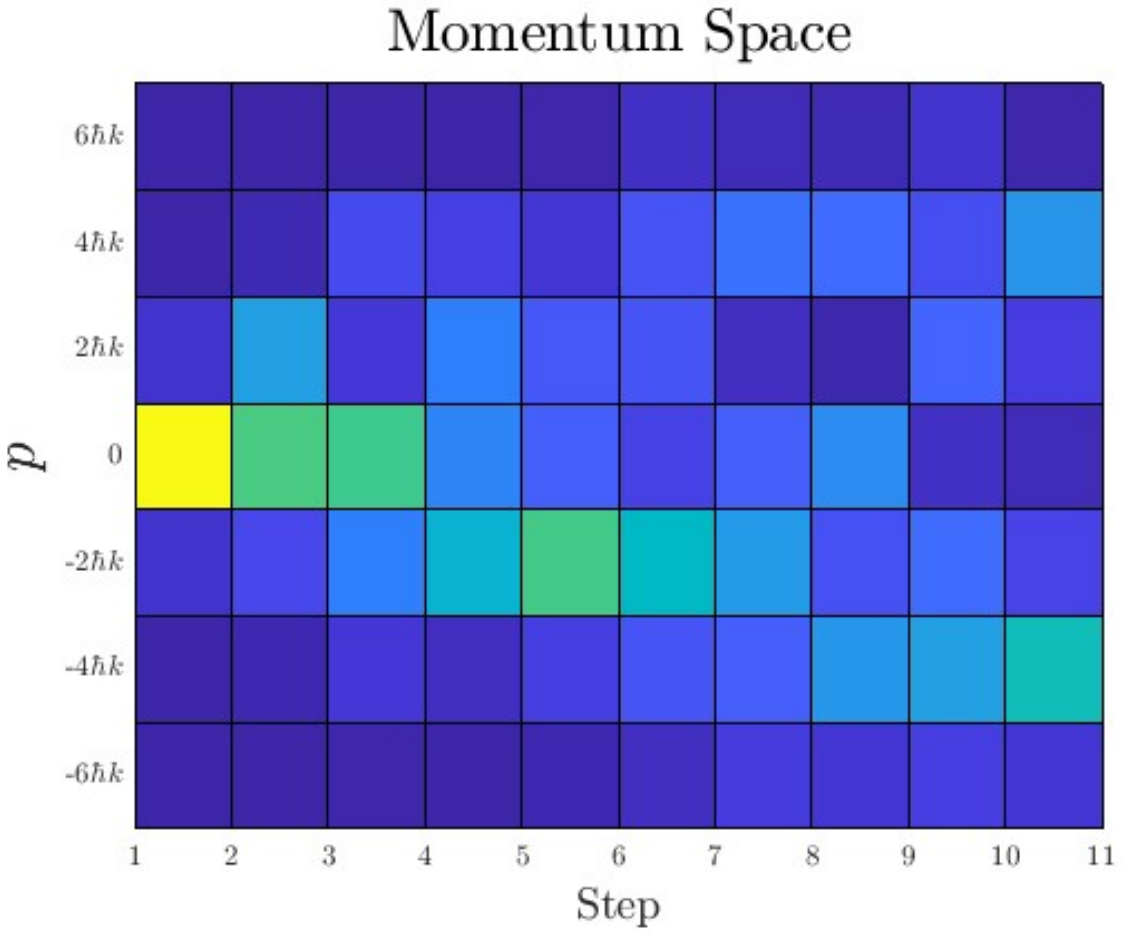

Figure 4.5: Evolution of the momentum space wave function as a function of time. Time is measured in steps along the x axis. The y axis is the momentum range of the wave function. The color intensity corresponds to the density of the wave function where bright yellow is high density and dark blue is low density.

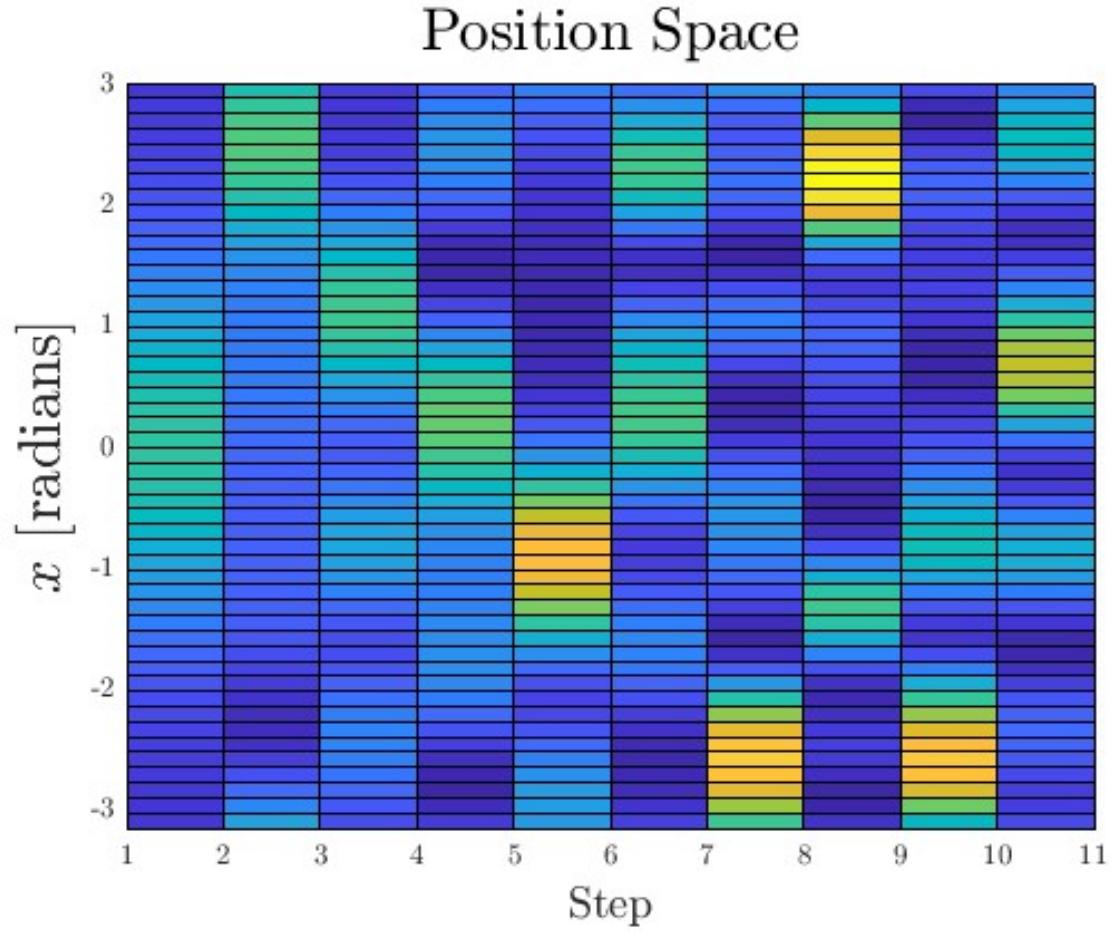

Figure 4.6: Evolution of the position space wave function as a function of time. Time is measured in steps along the x axis. The y axis is the spacial range of the lattice. The color intensity corresponds to the density of the wave function where bright yellow is high density and dark blue is low density.

Chapter 5

Mirror

The mirror component of the interferometer reflects the wave function in momentum space. Since this component acts on the wave once it has been split by the beamsplitter, the density is lower in each well and the mean field effects are lessened. In this project it is assumed that the mean field effects in this case are negligible. In section 5.2 we will show that this is the case. Thus, a non-interacting model is used to calculate the shaking function for the mirror component of the interferometer.

5.1 Lattice and Environment

The mirror version of the machine learning algorithm is in momentum space and the learning is done on a unitary instead of the wave function. The reason for this is that a general mirror should have the effect of reflecting any general wave function rather than transforming it into a specific wave-function. We use the same method with the target as a unitary of all zeros with off diagonal ones in the top right and bottom left corners. This unitary will flip the wave-function in momentum space. The feature and fidelity of the learning algorithm are also different from the beamsplitter. The fidelity is the channel fidelity given as

$$F = \frac{1}{d_s(d_s+1)}[Tr(MM^\dagger) + |Tr(M)|^2].[4] \tag{5.1}$$

The feature is similar to the feature in the beamsplitter lattice. Again, the goal is to describe the parity of the wave-function to the actor. Now, we want to note the parity of the result of the

unitary acting on the wave function. The feature is thus the parity of the unitary acting on the even and odd components of the wave-function.

5.2 Mean Field Effects

The mirror should have the function of reflecting the wave in both momentum and position space. We will first show the noninteracting case to verify that the mirror function has the expected action. The following mirror sequence is acted on the split wave-function.

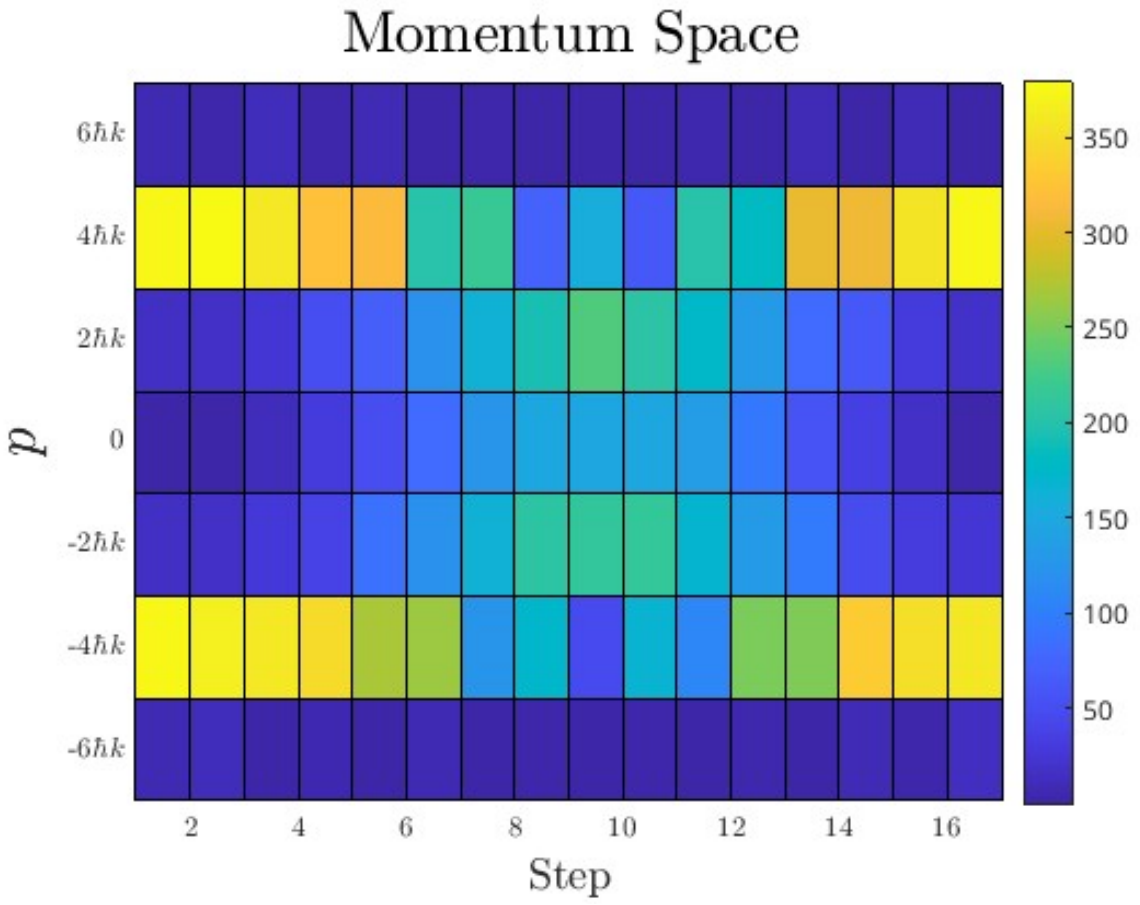

Figure 5.1: Evolution of the momentum space wave function as a function of time. Time is measured in steps along the x axis. The y axis is the spacial range of the lattice. The color intensity corresponds to the density of the wave function where bright yellow is high density and dark blue is low density.

The shaking function used in this simulation is shown in fig. 5.2. It was generated from the

non-interacting case via the methods described above and has a fidelity of 97.7%.

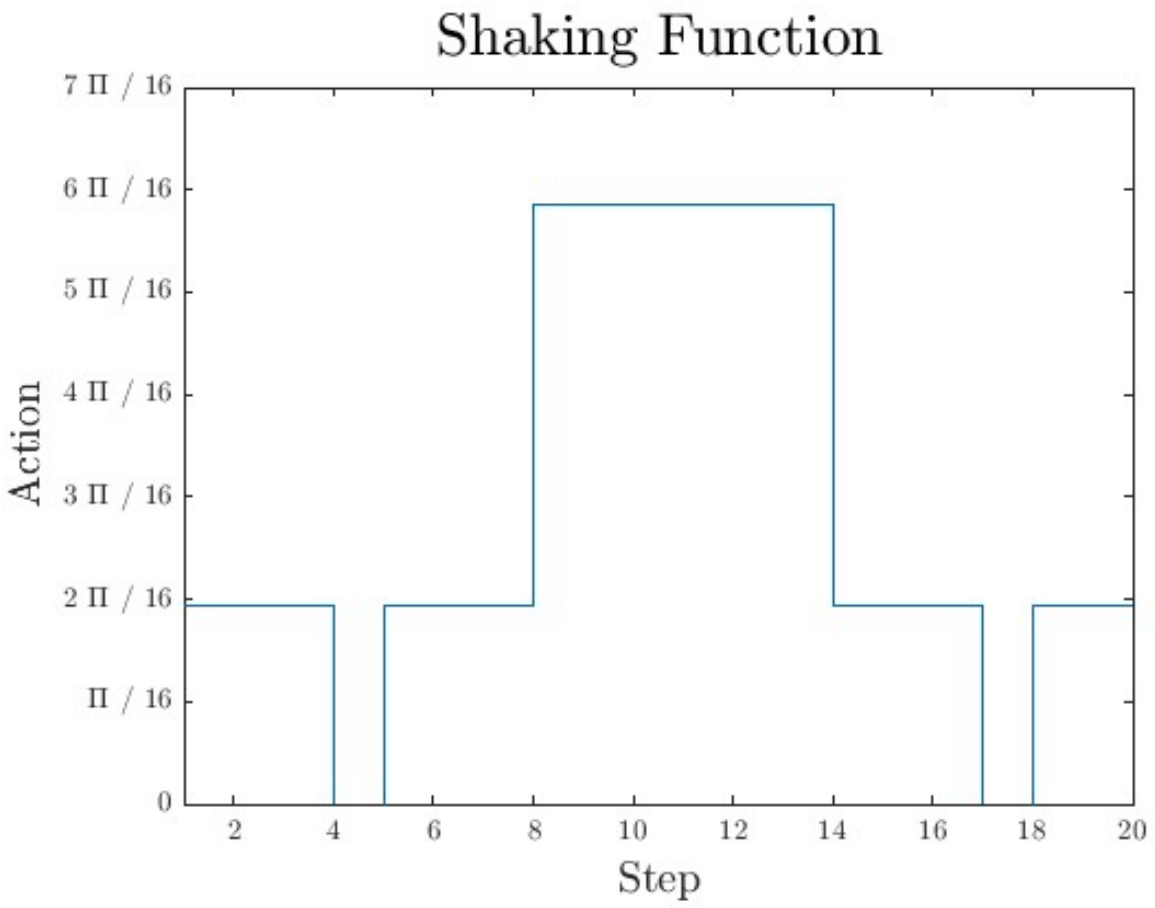

Figure 5.2: Non-interacting shaking function for mirror sequence

It can be seen in fig. 5.1 that the initial wave-function is slightly more dense in the $-4\hbar k$ component than the $4\hbar k$ component. At the end of the shaking sequence, it can be seen that the resulting wave-function is more dense in the $4\hbar k$ component than the $-4\hbar k$ component. This is the expected result of the reflection in momentum space. The initial fidelity of the state was 99.5% and was 99.8% after the mirror sequence.

We will now show the effects of the mean field interactions on the mirror sequence. As can be seen in fig. 5.1, the mirror has a similar action independent of the mean field effects. With interaction strength 2, the fidelity went from 99.5% to 98.9% after the mirror sequence. With interaction strength 5, the fidelity went from 99.4% to 98.9% after the mirror sequence. With

interaction strength 5, the fidelity went from 99.3% to 97.6% after the mirror sequence. This shows that the mean field effects are very small on the mirror sequence as was expected.

a	b
1 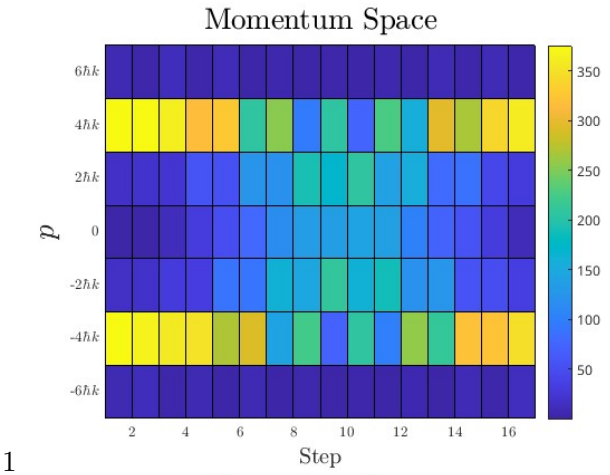	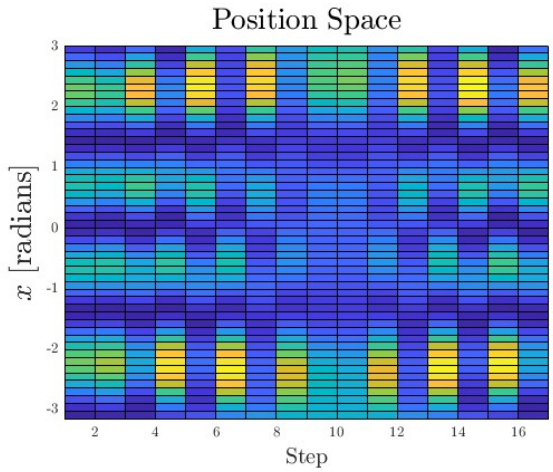
2 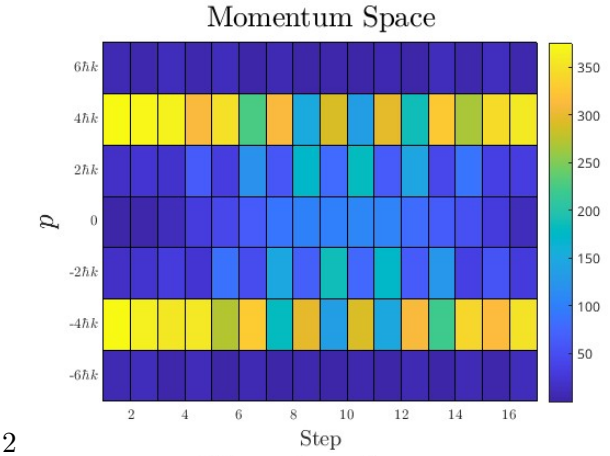	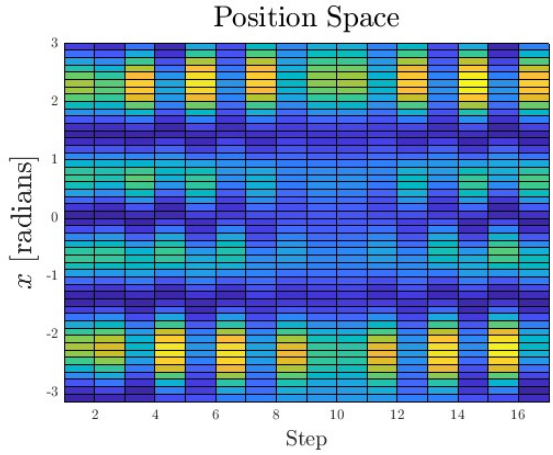
3 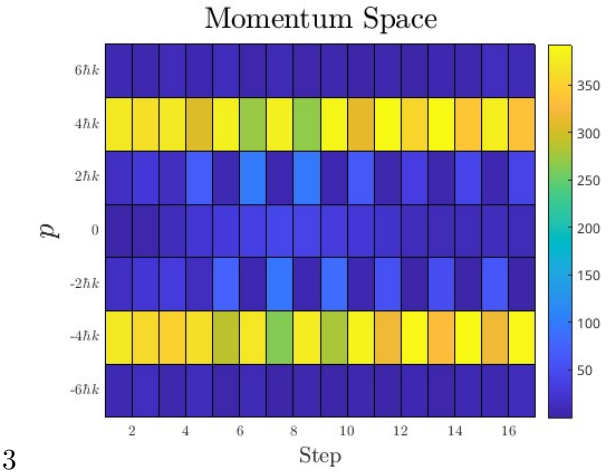	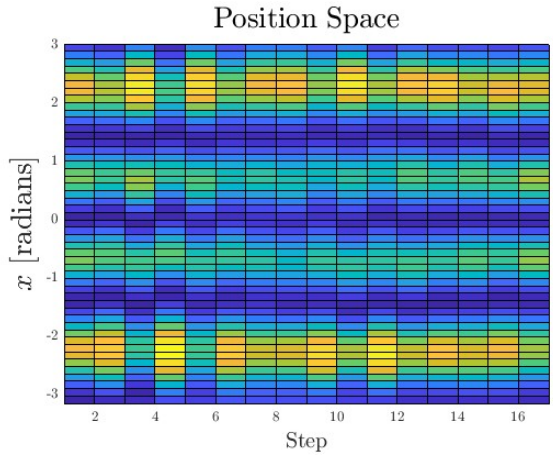

Table 5.1: Non-interacting mirror solution under varying interactions strengths. a) varying interaction strengths in momentum space. b) varying interaction strengths in position space. 1) interaction strength 2. 2) interaction strength 5. 3) interaction strength 10.

Chapter 6

Interferometer and Measurment

6.1 Sequence and Components

The interferometer sequence is comprised of the beamsplitter, mirror, and recombiner shaking functions. The recombiner function is defined as the reverse of the beamsplitter shaking function. This is the case because the time reversal property of the Gross-Pitaevskii equation allows us to undo the actions of the beamsplitter by applying the action in the opposite order.[8] The noninteracting shaking function for the interferometer is shown in fig. 6.1. It can be seen that the interval 30 to 40 is the reflection of the interval 0 to 10.

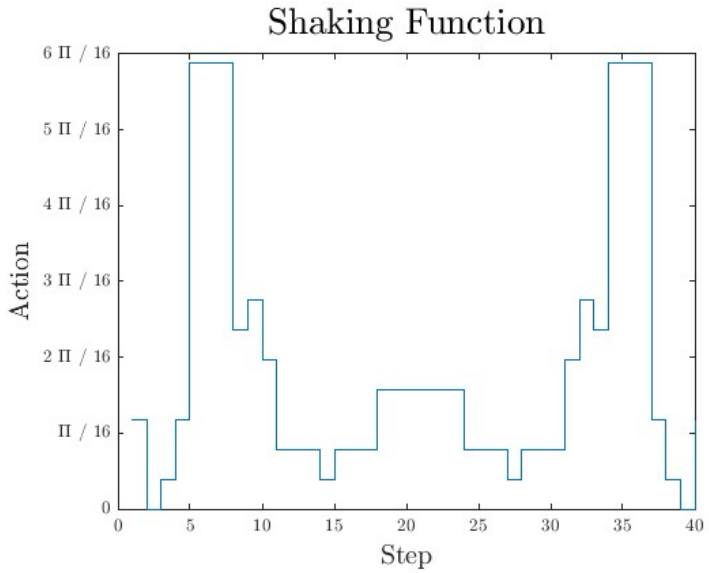

Figure 6.1: Shaking function of interferometer learned on the non-interacting model

The noninteracting interferometer is shown in momentum space in fig. 6.2. It can be seen that the mean field effects become more apparent in the higher scattering cases. In fig. 6.1, the interferometer is shown to decrease in fidelity as interaction strength increases. The shape of the interferometer in momentum space becomes blurry and there is a weaker peak at the final action.

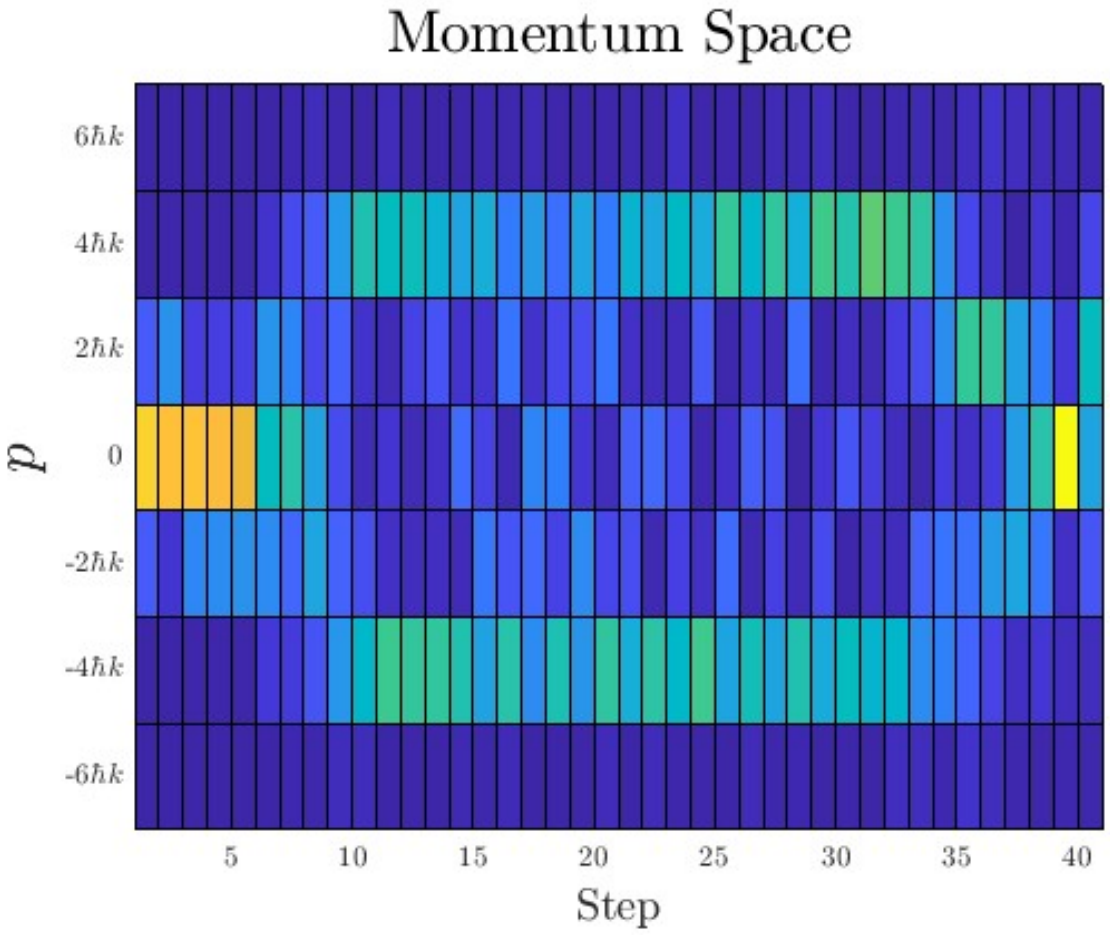

Figure 6.2: Non-interacting interferometer in momentum space. The x axis is time measured in steps. The x axis is momentum and the color represents the density of the wave-function with yellow indicating high density.

6.2 Interacting Interferometer

The interacting interferometer is generated in the same way as the non-interacting interferometer but with an interacting beamsplitter shaking function. The shaking sequence is shown in fig. 6.3 and was generated with an interaction strength of 10 dimensionless units. The first 10

steps are the beamsplitter sequence and the final ten steps are the recombiner, the reverse of the beamsplitter sequence. The 14 steps in the center are the mirror shaking function. This mirror function could be the same across the non-interacting and interacting models in theory. This function is different from the one shown previously because the frequency of the trap was changed in this learning cycle.

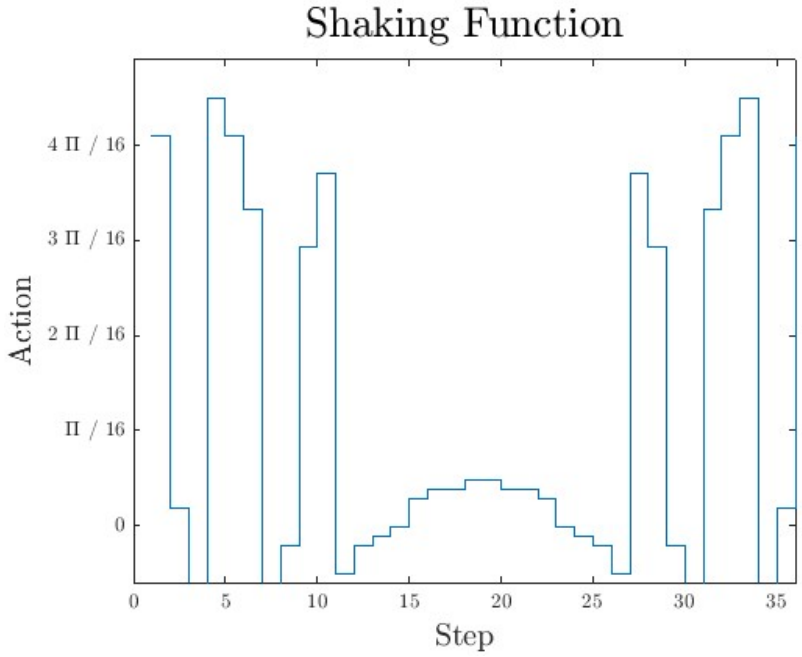

Figure 6.3: Shaking function determined by the reinforcement learning algorithm. The x axis is the step number and the y axis is the phase shift in radians.

The momentum space plot of the evolution of the interacting interferometer is shown in fig. 6.4. This shows the simulation of the interacting model with the interacting interferometer shaking function. In the final step there is a clear peak in the ground state momentum. This shows that it is possible to account for interactions in the learning cycle and maintain a high fidelity interferometer.

6.3 Measuring Acceleration

The interferometer is used to measure acceleration by observing a fringe pattern. Under zero acceleration, the fringe should look like the last action in the interferometer sequence. We

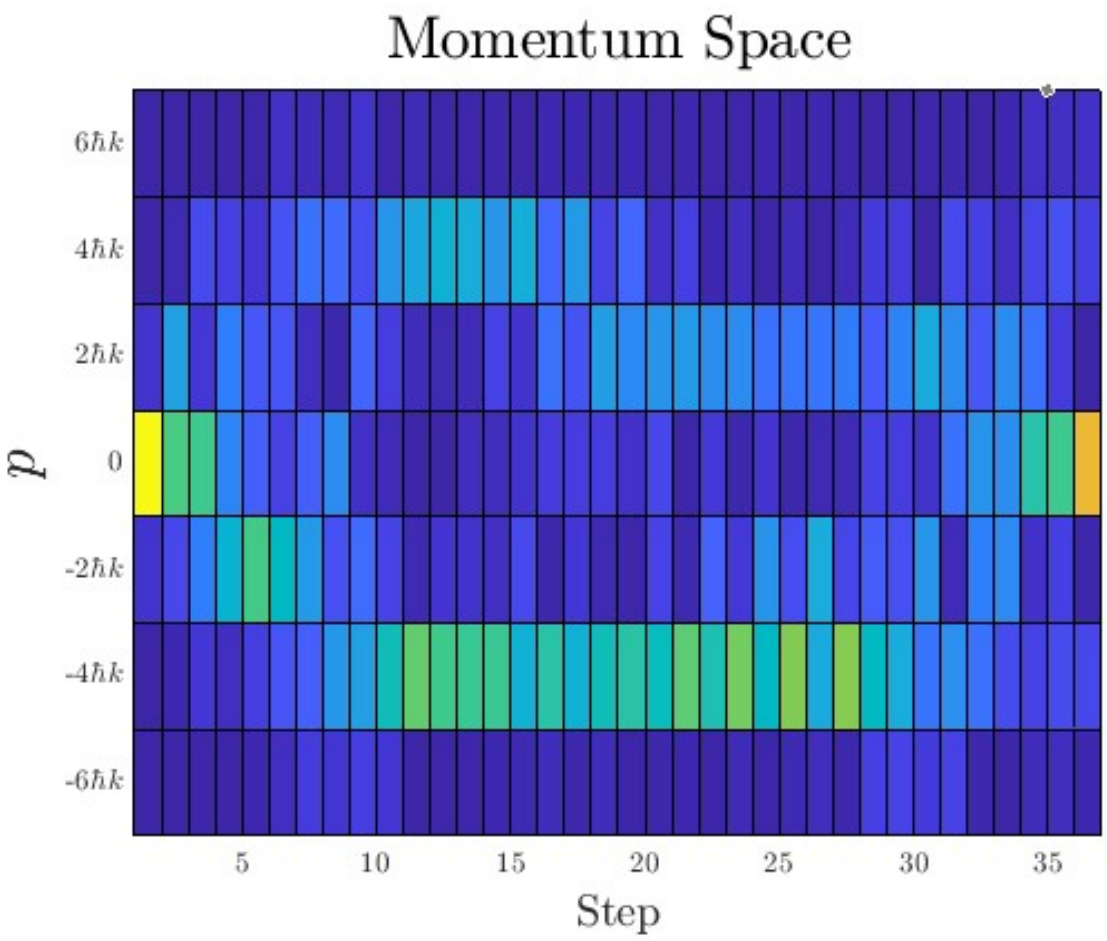

Figure 6.4: Evolution of the momentum space wave function as a function of time. Time is measured in steps along the x axis. The y axis is the momentum range of the wave function. The color intensity corresponds to the density of the wave function where bright yellow is high density and dark blue is low density.

can model the acceleration as a quadratically increasing phase shift in time imposed to the lattice. By implementing this model, we can simulate the fringe patterns that we expect to see under different magnitudes of acceleration. A plot of this is shown in fig. 6.6 for the learning solution and simulations with scattering 10.

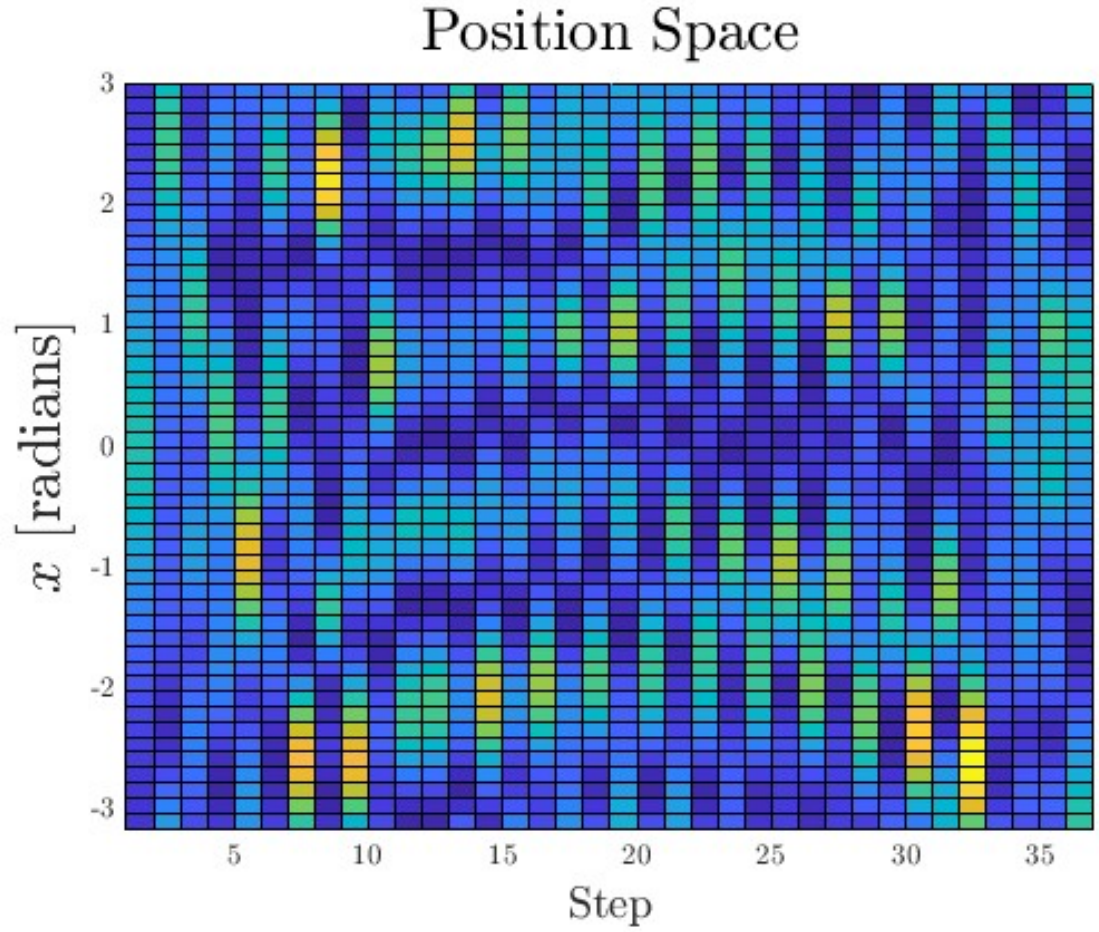

Figure 6.5: Evolution of the position space wave function as a function of time. Time is measured in steps along the x axis. The y axis is the spacial range of the lattice. The color intensity corresponds to the density of the wave function where bright yellow is high density and dark blue is low density.

	a	b
1	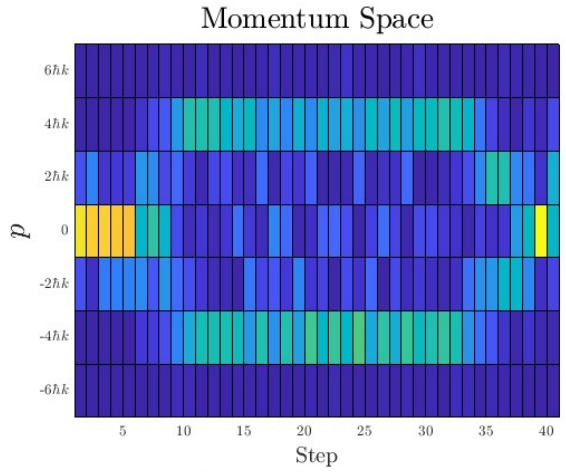	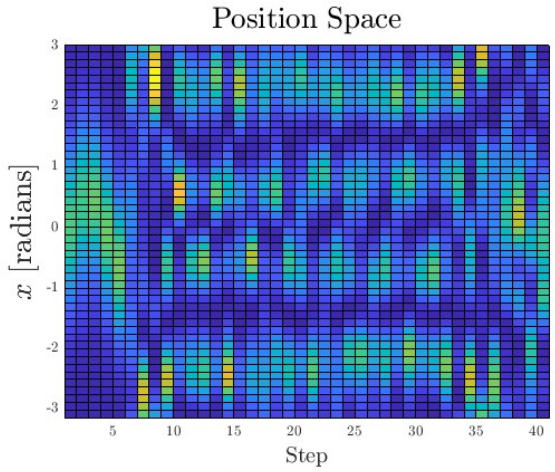
2	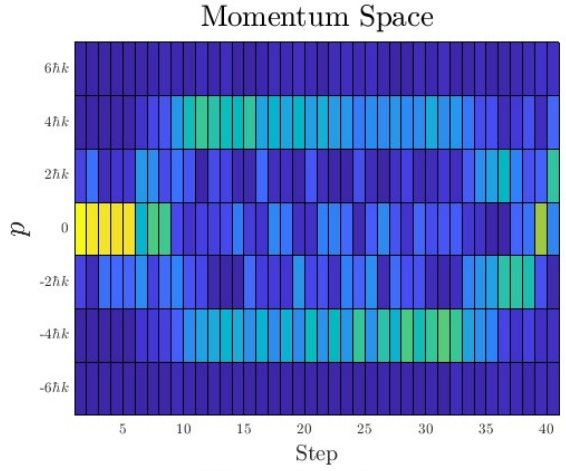	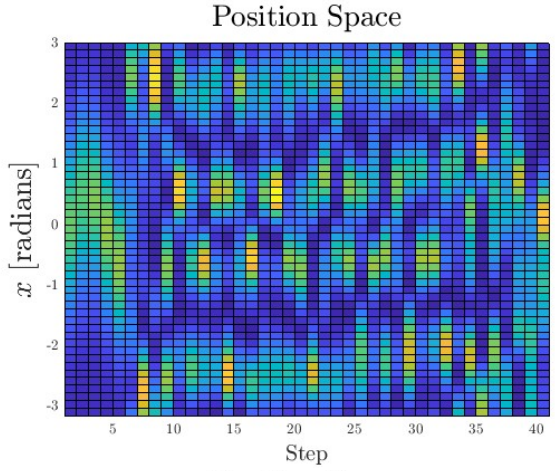
3	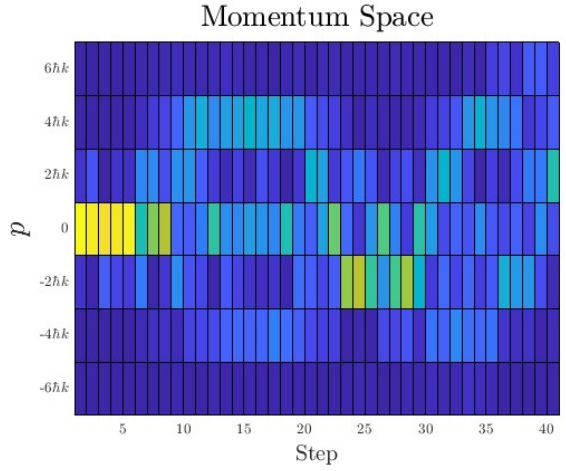	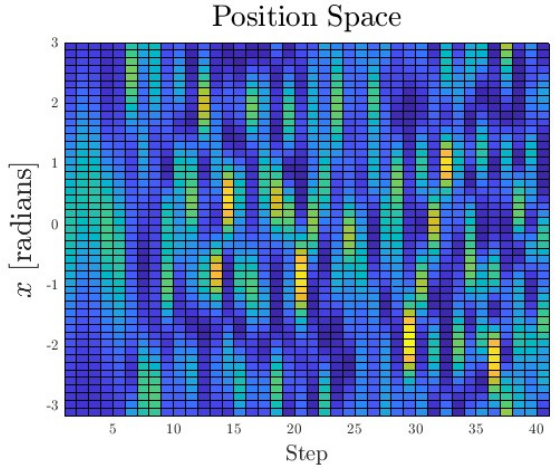

Table 6.1: Non-interacting interferometer solution under varying interactions strengths. a) varying interaction strengths in momentum space. b) varying interaction strengths in position space. 1) interaction strength 2. 2) interaction strength 5. 3) interaction strength 10.

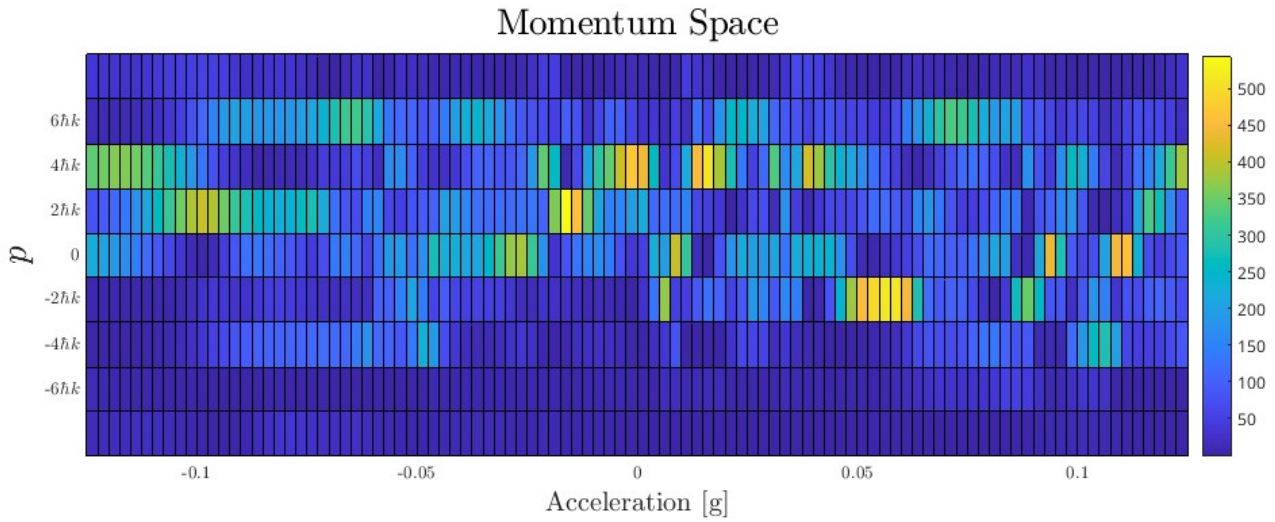

Figure 6.6: The different fringe patterns, shown in momentum space, that will be measured as a result of varying acceleration. The x axis is acceleration measured in units of gravity. The y axis is different values of momentum. The color represents the density of the wave-function.

Chapter 7

Conclusion

Shaken lattice matter-wave interferometry is a viable method to achieve high fidelity measurements of acceleration. The mean-field effects do lower the fidelity when they become strong enough. It is of interest to model these effects and account for them if the interaction strength is high. It is possible to generate shaking functions for the interacting model using reinforcement learning and the Gross-Pitaevskii equation. The study of interactions in shaken lattice interferometry would benefit from further research in characterization of effects of interaction strength and properties of BECs.

Bibliography

[1] Junaid Aasi, Joan Abadie, BP Abbott, Richard Abbott, TD Abbott, MR Abernathy, Carl Adams, Thomas Adams, Paolo Addesso, RX Adhikari, et al. Enhanced sensitivity of the ligo gravitational wave detector by using squeezed states of light. Nature Photonics, 7(8):613–619, 2013.

[2] Tobias Bothwell, Colin J. Kennedy, Alexander Aeppli, Dhruv Kedar, John M. Robinson, Eric Oelker, Alexander Staron, and Jun Ye. Resolving the gravitational redshift across a millimetre-scale atomic sample. Nature, 602(7897):420–424, Feb 2022.

[3] O. Carnal and J. Mlynek. Young's double-slit experiment with atoms: A simple atom interferometer. Phys. Rev. Lett., 66:2689–2692, May 1991.

[4] Liang-Ying Chih and Murray Holland. Reinforcement-learning-based matter-wave interferometer in a shaken optical lattice. Phys. Rev. Res., 3:033279, Sep 2021.

[5] Alexander D. Cronin, Jörg Schmiedmayer, and David E. Pritchard. Optics and interferometry with atoms and molecules. Rev. Mod. Phys., 81:1051–1129, Jul 2009.

[6] Vittorio Giovannetti, Seth Lloyd, and Lorenzo Maccone. Advances in quantum metrology. Nature photonics, 5(4):222–229, 2011.

[7] Jing Liu, Haidong Yuan, Xiao-Ming Lu, and Xiaoguang Wang. Quantum fisher information matrix and multiparameter estimation. Journal of Physics A: Mathematical and Theoretical, 53(2):023001, 2020.

[8] J. Martin, B. Georgeot, and D. L. Shepelyansky. Time reversal of bose-einstein condensates. Phys. Rev. Lett., 101:074102, Aug 2008.

[9] Lev Petrovic Pitaevskij and S. Stringari. Bose-Einstein condensation. Clarendon Press, 2003.

[10] Ben Stray, Andrew Lamb, Aisha Kaushik, Jamie Vovrosh, Anthony Rodgers, Jonathan Winch, Farzad Hayati, Daniel Boddice, Artur Stabrawa, Alexander Niggebaum, et al. Quantum sensing for gravity cartography. Nature, 602(7898):590–594, 2022.